This article was downloaded by: [Renmin University of China]
On: 13 October 2013, At: 10:45
Publisher: Taylor & Francis
Informa Ltd Registered in England and Wales Registered Number: 1072954 Registered office: Mortimer House, 37-41 Mortimer Street, London W1T 3JH, UK

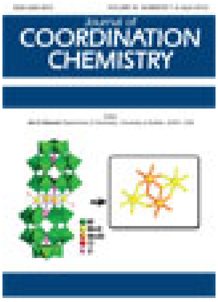

Journal of Coordination Chemistry
Publication details, including instructions for authors and subscription information:
http://www.tandfonline.com/loi/gcoo20

Synthesis, spectroscopic investigation, structural characterization, and DFT calculations of $[ReX_2(N_2COPh)(CH_3PhCN)(PPh_3)_2]$ (X=Cl, Br)

S. Michalik [a]

[a] Department of Inorganic and Coordination Chemistry, Institute of Chemistry, University of Silesia, 9th Szkolna St., 40-006 Katowice, Poland

Published online: 21 Mar 2012.

To cite this article: S. Michalik (2012) Synthesis, spectroscopic investigation, structural characterization, and DFT calculations of $[ReX_2(N_2COPh)(CH_3PhCN)(PPh_3)_2]$ (X=Cl, Br), Journal of Coordination Chemistry, 65:7, 1189-1200, DOI: 10.1080/00958972.2012.669036

To link to this article: http://dx.doi.org/10.1080/00958972.2012.669036

PLEASE SCROLL DOWN FOR ARTICLE

Taylor & Francis makes every effort to ensure the accuracy of all the information (the "Content") contained in the publications on our platform. However, Taylor & Francis, our agents, and our licensors make no representations or warranties whatsoever as to the accuracy, completeness, or suitability for any purpose of the Content. Any opinions and views expressed in this publication are the opinions and views of the authors, and are not the views of or endorsed by Taylor & Francis. The accuracy of the Content should not be relied upon and should be independently verified with primary sources of information. Taylor and Francis shall not be liable for any losses, actions, claims, proceedings, demands, costs, expenses, damages, and other liabilities whatsoever or howsoever caused arising directly or indirectly in connection with, in relation to or arising out of the use of the Content.

This article may be used for research, teaching, and private study purposes. Any substantial or systematic reproduction, redistribution, reselling, loan, sub-licensing, systematic supply, or distribution in any form to anyone is expressly forbidden. Terms &

Journal of Coordination Chemistry
Vol. 65, No. 7, 10 April 2012, 1189–1200

Taylor & Francis
Taylor & Francis Group

Synthesis, spectroscopic investigation, structural characterization, and DFT calculations of $[ReX_2(N_2COPh)(CH_3PhCN)(PPh_3)_2]$ (X = Cl, Br)

S. MICHALIK*

Department of Inorganic and Coordination Chemistry, Institute of Chemistry, University of Silesia, 9th Szkolna St., 40-006 Katowice, Poland

(*Received 18 October 2011; in final form 2 January 2012*)

Reactions of $[ReX_2(\eta^2\text{-}N_2COPh\text{-}N',O)(PPh_3)_2]$ with 3-methylbenzonitrile give two isostructural complexes, $[ReX_2(N_2COPh)(CH_3PhCN)(PPh_3)_2]$ (X = Cl, Br). The crystal and molecular structures of $[ReCl_2(N_2COPh)(CH_3PhCN)(PPh_3)_2]$ (**1**) and $[ReBr_2(N_2COPh)(CH_3PhCN)(PPh_3)_2] \cdot CH_2Cl_2$ (**2**) were determined. The electronic structures were examined with density functional theory (DFT). The spin-allowed electronic transitions were calculated with the time-dependent DFT method, and the UV-Vis spectrum has been discussed.

Keywords: Rhenium; X-ray structure; Electronic structure; Nitrile

1. Introduction

The coordination chemistry of rhenium is of growing interest from synthetic aspects, structural, physicochemical properties, and reactivity, as well as applications to radiotherapeutic cancer agents, materials chemistry, nitrogen fixation, and catalysis [1]. The ^{186}Re (1.07 MeV β-emitter, $t_{1/2}$ 90 h) and ^{188}Re (2.12 MeV β-emitter, $t_{1/2}$ 17 h) are among the most attractive isotopes for therapeutic applications. For example ^{188}Re is in demand for a variety of research and clinical applications, including treatment of metastatic bone cancer, non-resectable liver cancer, non-melanoma skin cancer, treatment of arthritis, and inhibition of arterial restenosis following balloon angioplasty [2–5]. Diazenido complexes are important because of their significance in nitrogen fixation [6–8]. The diazenido complexes, for example, $[ReCl_2(N_2COPh)(Hpz)(PPh_3)_2]$ (Hpz = pyrazole), $[ReCl_2(N_2COPh)(Hpz)_2(PPh_3)]$, $[ReClF(N_2COPh)(Hpz)_2(PPh_3)]$, and their precursors $[ReX_2(\eta^2\text{-}N_2COPh\text{-}N',O)(PPh_3)_2]$ (X = Cl, Br) act as selective catalysts in a single-pot process for oxidation of ethane [9]. The complexes $[ReCl(NNAr)_2(PPh_3)_2]$ (Ar = 4-substituted phenyl) form efficient catalysts for metathesis and ring-opening metathesis polymerization [10].

This article is focused on examination of the reaction of $[ReX_2(\eta^2\text{-}N_2COPh\text{-}N',O)(PPh_3)_2]$ with 3-methylbenzonitrile, presenting the synthesis and spectroscopic

---

*Email: smich1@wp.pl

Journal of Coordination Chemistry
ISSN 0095-8972 print/ISSN 1029-0389 online © 2012 Taylor & Francis
http://dx.doi.org/10.1080/00958972.2012.669036

data for $[ReCl_2(N_2COPh)(CH_3PhCN)(PPh_3)_2]$ (**1**) and $[ReBr_2(N_2COPh)(CH_3PhCN)(PPh_3)_2] \cdot CH_2Cl_2$ (**2**) with *cis* halides and *trans* triphenylphosphines. X-ray studies have been performed for **1** and **2**, and electronic structures have been calculated with density functional theory (DFT). The spin-allowed singlet–singlet electronic transitions of $[ReX_2(N_2COPh)(CH_3PhCN)(PPh_3)_2]$ have been calculated with time-dependent DFT method (TDDFT). The UV-Vis spectrum of $[ReCl_2(N_2COPh)(CH_3PhCN)(PPh_3)_2]$ has been discussed on this basis.

2. Experimental

2.1. *General procedure*

Ammonium perrhenate and triphenylphosphine were purchased from Aldrich Chemical, 3-methylbenzonitrile was purchased from Fluka AG; all were used without purification. $[ReX_2(\eta^2\text{-}N_2COPh\text{-}N',O)(PPh_3)_2]$ was prepared according to the literature method [11, 12]. The solvent used in the reaction was argon saturated.

2.2. *Synthesis of $[ReCl_2(N_2COPh)(CH_3PhCN)(PPh_3)_2]$* (1)

$[ReCl_2(\eta^2\text{-}N_2COPh\text{-}N',O)(PPh_3)_2]$ (1 g, 1.1 mmol) was added to 3-methylbenzonitrile (0.2 g, 1.7 mmol) suspended in acetone (50 mL) and stirred at room temperature for 48 h. The brown crystalline precipitate of **1** was collected by filtration. The product was washed with Et_2O (3*10 mL). Crystals suitable for X-ray structure determination were obtained by recrystallization from a mixture of chloroform and dichloromethane (1 : 1, v/v). Yield: 0.97 g 87%. IR (KBr): 3264 ν_{ArH}; 3056 ν_{CH}; 2246 $\nu_{C=N}$; 1640 $\nu_{NN\text{–}CO}$; 1577, 1507 $\nu_{(C=C)}$; 1482, 1307 $\delta_{(C\text{–}CH\text{ in the plane})}$; 1434 $\nu_{Ph(P\text{–}Ph)}$; 1230 $\nu_{(C\text{–}C(O)NN)}$; 1092, 1017 $\delta_{(C\text{–}CH\text{ in the plane})}$; 743 $\delta_{(C\text{–}C\text{ out of the plane})}$; 692 $\delta_{(C\text{–}C\text{ in the plane})}$; 518, 497 $\nu_{(Re\text{–}NNC(O)Ph)}$. UV-Vis (methanol; nm): 510, 378, 277, 250, 211. ^1H NMR (δ, $CDCl_3$): 7.871 (Ph–C(O)NN), 7.624–7.203 (PPh_3), 6.714 (C_6H_4–CN), 2.309 (CH_3). ^{31}P NMR (δ, $CDCl_3$): –4.266, –2.376 (s, PPh_3). Anal. Calcd for $C_{51}H_{42}Cl_2N_3OP_2Re$: C, 59.36; H, 4.10; N, 4.07. Found (%): C, 59.40; H, 4.12; N, 4.12.

2.3. *Synthesis of $[ReBr_2(N_2COPh)(CH_3PhCN)(PPh_3)_2] \cdot CH_2Cl_2$ (2)*

A procedure similar to that for $[ReCl_2(N_2COPh)(CH_3PhCN)(PPh_3)_2]$ was used with $[ReBr_2(\eta^2\text{-}N_2COPh\text{-}N',O)(PPh_3)_2]$ (1 g, 1 mmol) and 3-methylbenzonitrile (0.2 g, 1.7 mmol). The brown crystalline precipitate of **2** was collected by filtration. The product was washed with Et_2O (3*10 mL). Crystals suitable for X-ray structure determination were obtained by recrystallization from a mixture of chloroform and dichloromethane (1 : 1, v/v). Yield: 1.07 g 90%. IR (KBr): 3266 ν_{ArH}; 3057 ν_{CH}; 2244 $\nu_{C=N}$; 1644 $\nu_{NN\text{–}CO}$; 1572, 1513 $\nu_{(C=C)}$; 1482, 1308 $\delta_{(C\text{–}CH\text{ in the plane})}$; 1433 $\nu_{Ph(P\text{–}Ph)}$; 1229 $\nu_{(C\text{–}C(O)NN)}$; 1090, 1015 $\delta_{(C\text{–}CH\text{ in the plane})}$; 742 $\delta_{(C\text{–}C\text{ out of the plane})}$; 692 $\delta_{(C\text{–}C\text{ in the plane})}$; 518, 498 $\nu_{(Re\text{–}NNC(O)Ph)}$. UV-Vis (methanol; nm): 530, 382, 257, 211. ^1H NMR (δ, $CDCl_3$): 7.911 (Ph–C(O)NN), 7.597–7.179 (PPh_3), 6.703 (C_6H_4–CN), 5.419 (CH_2), 2.311 (CH_3). ^{31}P NMR (δ, $CDCl_3$): –7.731, –4.272 (s, PPh_3). Anal. Calcd for $C_{52}H_{44}Br_2Cl_2N_3OP_2Re$: C, 51.80; H, 3.68; N, 3.48. Found (%): C, 51.82; H, 3.70; N, 3.50.

2.4. *Physical measurements and DFT calculations*

Infrared (IR) spectra were recorded on a Nicolet Magna 560 spectrophotometer from 4000 to 400 cm^{-1} with the samples in the form of potassium bromide pellets. Electronic spectra were measured on a Lab Alliance UV-Vis 8500 spectrophotometer from 180 to 600 nm in methanol. ^1H and ^{31}P NMR spectra were obtained at room temperature in $CDCl_3$ using a Bruker 400 spectrometer. Elemental analyses (C, H, and N) were performed on a Perkin-Elmer CHN-2400 analyzer.

The calculations were carried out using the Gaussian 09 program [13]. The DFT/B3LYP [14, 15] method was used for geometry optimization and electronic structure determination. Electronic spectra were calculated by the TDDFT method [16] with use of the CAM-B3LYP functional [17]. The calculations were performed using the Lanl2dz basis set [18] on rhenium and bromine and polarization functions for all other atoms: 6–31 G** for chlorine, carbon, nitrogen, oxygen, and 6–31 G for hydrogen. The PCM solvent model was used in the Gaussian calculations with methanol as solvent. Natural bond orbital (NBO) calculations were performed with the NBO code included in Gaussian 09. GaussSum 2.2 [19] was used to calculate group contributions to the molecular orbitals and to prepare the partial density of states (DOS) and overlap population DOS (OPDOS) spectra. The contribution of a group to a molecular orbital was calculated using Mulliken population analysis. PDOS and OPDOS spectra were created by convoluting the molecular orbital information with Gaussian curves of unit height and FWHM of 0.3 eV Mayer bond orders were calculated with use of QMForge program [20].

2.5. *Crystal structure determinations and refinement*

Crystals of $[ReCl_2(N_2COPh)(CH_3PhCN)(PPh_3)_2]$ (**1**) and $[ReBr_2(N_2COPh)(CH_3PhCN)(PPh_3)_2]\cdot CH_2Cl_2$ (**2**) suitable for X-ray structure determination were obtained by recrystallization from a mixture of chloroform and dichloromethane.

Brown crystals of **1** and **2** were mounted on an Xcalibur, Atlas, Gemini Ultra Oxford Diffraction automatic diffractometer equipped with a CCD detector and used for data collection. X-ray intensity data were collected with graphite monochromated Mo-Kα radiation ($\lambda = 0.71073$ Å) at 295.0(2) K, with ω scan mode. Ewald sphere reflections were collected up to $2\theta = 50.10$. The unit cell parameters were determined from least-squares refinement of the setting angles of 14,594 and 24,009 strongest reflections for **1** and **2**, respectively. Details concerning crystal data and refinement are gathered in table 1. During the data reduction the decay correction coefficient was taken into account. Lorentz, polarization, and numerical absorption corrections were applied. The structures were solved by the Patterson method. All non-hydrogen atoms were refined anisotropically using full-matrix least-squares on F^2. The Olex2 [21] and SHELXS-97, SHELXL-97 [22] programs were used for all the calculations. Atomic scattering factors were those incorporated in the computer programs.

Table 1. Crystal data and structure refinement details of $[ReCl_2(N_2COPh)(CH_3PhCN)(PPh_3)_2]$ (**1**) and $[ReBr_2(N_2COPh)(CH_3PhCN)(PPh_3)_2] \cdot CH_2Cl_2$ (**2**).

	1	**2**
Empirical formula	$C_{51}H_{42}Cl_2N_3OP_2Re$	$C_{51}H_{42}Br_2N_3OP_2Re$, CH_2Cl_2
Formula weight	1031.92	1205.76
Temperature (K)	295.0(2)	295.0(2)
Crystal system	Monoclinic	Monoclinic
Space group	$P2_1/n$	$P2_1/n$
Unit cell dimensions (Å, °)		
a	12.8918(7)	13.0313(3)
b	17.9560(10)	18.9375(4)
c	20.4005(11)	20.5785(6)
α	90	90
β	100.644(5)	101.361(2)
γ	90	90
Volume (Å^3), Z	4641.2(4), 4	4978.9(2), 4
Calculated density (Mg m^{-3})	1.477	1.609
Absorption coefficient (mm^{-1})	2.842	4.257
F(000)	2064	2376
Crystal size (mm^3)	$0.14 \times 0.11 \times 0.07$	$0.20 \times 0.11 \times 0.09$
θ range for data collection (°)	3.38–25.05	3.38–25.05
Limiting indices	$-15 \le h \le 15$; $-21 \le k \le 21$; $-24 \le l \le 23$	$-15 \le h \le 15$; $-22 \le k \le 22$; $-24 \le l \le 24$
Reflections collected	35,650	46,976
Independent reflections	8214 [R(int) = 0.0387]	8807 [R(int) = 0.0320]
Data/restraints/parameters	8214/0/542	8807/0/569
Goodness-of-fit on F^2	1.054	1.044
Final R indices [$I > 2\sigma(I)$]	$R_1 = 0.0362$, $wR_2 = 0.0840$	$R_1 = 0.0327$, $wR_2 = 0.0766$
R indices (all data)	$R_1 = 0.0546$, $wR_2 = 0.0900$	$R_1 = 0.0448$, $wR_2 = 0.0787$
Largest difference peak and hole (e Å^{-3})	1.418 and –0.826	1.381 and –0.717

3. Results and discussion

3.1. *Preparation and IR data*

Reactions of $[ReX_2(\eta^2\text{-}N_2COPh\text{-}N',O)(PPh_3)_2]$ (X = Cl, Br) with CH_3PhCN result in opening of the chelate ring through displacement of coordinated carbonyl by 3-methylbenzonitrile and lead to $[ReX_2(N_2COPh)(CH_3PhCN)(PPh_3)_2]$:

$$[ReX_2(\eta^2\text{-}N_2COPh\text{-}N', O)(PPh_3)_2] + CH_3PhCN \\ \rightarrow [ReX_2(N_2COPh)(CH_3PhCN)(PPh_3)_2]\ (X = Cl, Br)$$

The products were isolated as brown microcrystalline solids, soluble in common organic solvents.

In contrast to $[ReX_2(\eta^2\text{-}N_2COPh\text{-}N',O)(PPh_3)_2]$ the IR spectra for **1** and **2** show several bands in the range 1550–1650 cm^{-1} assigned to ν(N=N), ν(C–N), and ν(C=O), which confirm the opening of the chelate ligand [23]. The complex contains triphenylphosphines and thus shows the characteristic pair of bands at approximately 1430 and 1480 cm^{-1} and typically the lower frequency band is more intense [24].

Table 2. Hydrogen bonds for **1** and **2**.

D	A	H···A	D···A	D–H···A
1				
C(7)	N(2)	2.47	2.791(7)	100.6
C(10)	O(1)	2.38	3.221(7)	150.0
C(21)	Cl(1)	2.72	3.450(7)	135.5
C(21)	Cl(2)	2.79	3.333(7)	118.7
C(23)	O(1)	2.51	3.414(7)	163.8
C(35)	Cl(2)	2.73	3.555(6)	148.7
C(45)	Cl(2)	2.72	3.576(7)	153.7
2				
C(35)	Br(1)	2.85	3.614(7)	140.7
C(29)	Br(2)	2.84	3.705(6)	155.0
C(21)	Br(2)	2.82	3.556(6)	137.2
C(10)	O(1)	2.58	3.323(9)	136.8
C(7)	N(2)	2.45	2.791(8)	101.8

The ^{1}H NMR spectra of [ReCl$_2$(N$_2$COPh)(CH$_3$PhCN)(PPh$_3$)$_2$] reveal resonances typical for aromatic protons of coordinated PPh$_3$, N$_2$C(O)Ph, and 3-methylbenzonitrile [25, 26]. The lack of paramagnetic shift broadening of resonances in the ^{1}H NMR spectra of **1** and **2** confirms diamagnetism of the complex. In the ^{31}P NMR spectra of the complexes two singlets at –4.266, –2.376 ppm and –7.731, –4.272 ppm indicate the PPh$_3$ ligands are not exactly *trans*, which is in agreement with the structures of the complexes. On the other hand, the monodentate Re–NNC(O)Ph in these complexes (see crystal structure) is not plane symmetrical. Thus, unless this ligand undergoes free rotation, which seems unlikely given the Re–N bond character, there is no reason to expect the two phosphines to be equivalent. Rather, it is suspected that this ligand does not rotate and so one phosphorous is in the neighborhood of the carbonyl oxygen, while the other is not. Thus, their electronic environments are different and this is reflected in the different chemical shifts observed. Therefore, the inequivalence of the two ^{31}P nuclei in the ^{31}P NMR spectrum results from steric and electronic factors.

3.2. *Crystal structures*

Both complexes are iso-structural in the solid state, crystallize in the monoclinic space group $P2_1/n$, and their structures consist of discrete and well-separated monomers. Intramolecular and intermolecular interactions strong enough to govern crystal packing or molecule conformation were not found in the structures of **1** and **2**. Only intermolecular short contacts which could be considered as weak hydrogen bonds were detected (table 2).

The molecular structures of **1** and **2** are presented in figure 1 and selected bond distances and angles are collected in table 3. The complexes show octahedral coordination geometry. The rhenium center exhibits mutually *trans* triphenylphosphine molecules minimizing steric congestion and chloride/bromide *trans* to the monodentate organodiazenido and to 3-methylbenzonitrile which displaced the carbonyl oxygen of the diazenido substituent. Angular distortions from an ideal octahedron are caused by the presence of multiple bonding ligand (–NNR) in the *cis* position to 3-methylbenzonitrile. The Re(1)–N(1)–N(2) angles are essentially linear and the N(1)–N(2)–C angles

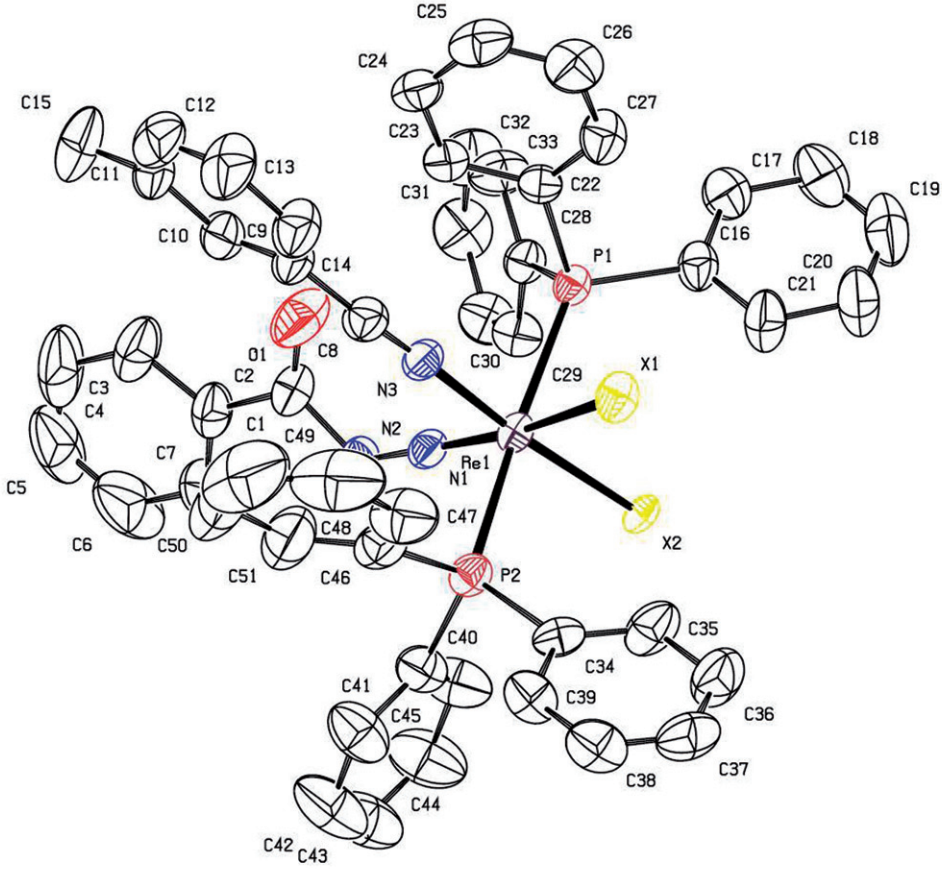

Figure 1. ORTEP drawing of [$ReX_2(N_2COPh)(CH_3PhCN)(PPh_3)_2$] with 50% probability displacement ellipsoids. Hydrogen atoms and solvent molecule are omitted for clarity.

are near 120°, indicating "singly bent" benzoyldiazenido complexes. The short Re–N(1) and N(1)–N(2) distances suggest extensive delocalization and multiple bonding throughout the N_2COPh unit and this observation is confirmed by the virtual planarity of the entire Re–N–NCOPh as well as linearity of the Re–N–N unit. The Re–N(1), N(1)–N(2), and N(2)–C bond lengths and N(1)–N(2)–C, Re–N(1)–N(2) angles are in good agreement with values found for other "singly bent" organodiazenido complexes [27, 28]. Significant lengthening of the Re–X bonds results from chloride/bromide *trans* to the strongly π-interacting benzoyldiazenido and 3-methylbenzonitrile. The Re–X(2) bond *trans* to the NNR ligand is shorter than the Re–X(1) bond *trans* to 3-methylbenzonitrile, which indicates stronger *trans* influence of 3-methylbenzonitrile in comparison with benzoyldiazenido. The Re–N(3) bond lengths (2.056(3) and 2.050(5) Å) are in agreement with analogous values found previously in similar rhenium compounds containing the organonitrile ligands [29, 30]. Both complexes have structures similar to those reported by Dilworth *et al.* [31] with aromatic hydrazines forming diazenides and with coordinated acetonitrile (similar to benzonitrile).

Table 3. Selected bond lengths (Å) and angles (°) for **1** and **2**.

	1		**2**	
	Exp	Calcd	Exp	Calcd
Re(1)–N(1)	1.749(2)	1.758	1.791(5)	1.759
Re(1)–N(3)	2.056(3)	2.036	2.050(5)	2.046
Re(1)–P(1)	2.463(9)	2.525	2.469(13)	2.541
Re(1)–P(2)	2.488(9)	2.525	2.465(14)	2.532
Re(1)–X(1)	2.424(9)	2.522	2.5797(6)	2.675
Re(1)–X(2)	2.416(8)	2.488	2.5656(6)	2.637
P(1)–Re(1)–P(2)	175.71(2)	174.73	174.18(4)	176.26
P(1)–Re(1)–N(1)	90.58(7)	91.88	93.40(14)	91.65
P(1)–Re(1)–N(3)	88.16(7)	91.81	90.90(13)	90.71
N(1)–Re(1)–N(3)	89.55(10)	91.56	90.94(18)	91.00
P(2)–Re(1)–N(1)	93.32(7)	91.78	92.41(14)	92.46
P(2)–Re(1)–N(3)	90.09(7)	91.87	88.64(13)	90.28
N(1)–Re(1)–X(1)	97.05(8)	97.38	92.20(13)	93.98
N(1)–Re(1)–X(2)	171.79(7)	170.64	172.90(13)	171.76
N(3)–Re(1)–X(1)	173.27(7)	171.06	176.48(13)	174.60
N(3)–Re(1)–X(2)	82.26(7)	79.09	82.19(13)	81.33
X(1)–Re(1)–X(2)	91.15(3)	87.86	94.72(2)	93.81
P(1)–Re(1)–X(1)	93.03(3)	91.98	90.50(3)	90.39
P(2)–Re(1)–X(1)	88.26(3)	88.53	89.64(3)	87.41
P(1)–Re(1)–X(2)	88.61(3)	87.86	84.93(3)	86.54
P(2)–Re(1)–X(2)	87.27(3)	87.86	89.26(3)	90.59

X denotes Cl in **1** and Br in **2**.

3.3. *Electronic structure*

To gain insight into the electronic structures and bonding properties of these complexes, DFT calculations were carried out. Before calculation of electronic structures, their geometries were optimized in triplet states using the B3LYP functional. From the data collected in table 3 one may see that the bond lengths are elongated by ~0.1 Å in the calculated gas phase structures and the change of bond angles does not exceed 3°. Figure 2 shows that calculated and experimental IR spectra of **1** are in good agreement.

The benzoyldiazenido ligand ($N_2C(O)Ph$) is a uni-negative four electron donor and the formal oxidation state of the rhenium in $[ReX_2(N_2C(O)Ph)(L)(PPh_3)_2]$ is assigned as +3. The atomic charges from the natural population analysis for the complexes show considerably lower values than the formal charge of +3 on rhenium (–0.6), corresponding to a d^4 configuration of the central ion. It results from significant charge donation from the ligands.

Mayer bond orders of Re–P, Re–$N_2C(O)Ph$, Re–N=C, and Re–X are similar in the complexes, 1.4, 2.7, 0.7, and 1.6 for chloride and 1.8 for bromide complexes, respectively. Bond orders between rhenium and nitrile ligands lower than 1 indicate ionic character in the bond. The value of the bond order between rhenium and diazenido confirms the considerable donor ability of the ligand and there is indication that the d^4 configuration of rhenium is probable.

The simplified diagrams of frontier molecular orbitals of the complexes are presented in figure 3. Among the occupied molecular orbitals of the complexes the largest numbers constitute orbitals of the PPh_3 and nitrile type ligands which are not relevant for the discussion. The d_{yz}, d_{xy}, d_{zx} orbitals of rhenium contribute to the highest

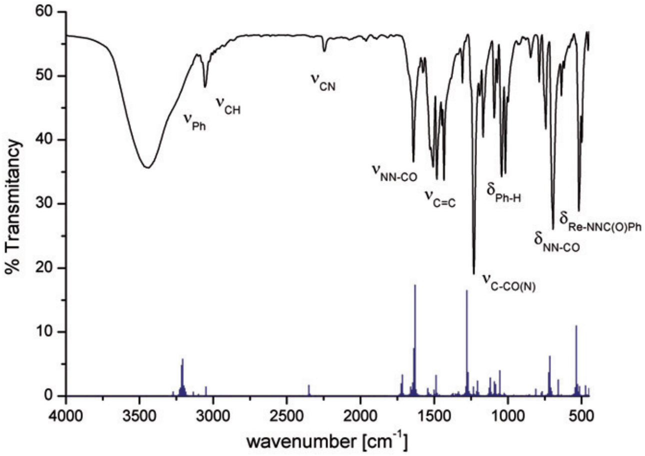

Figure 2. IR spectrum of [ReCl$_2$(N$_2$COPh)(CH$_3$PhCN)(PPh$_3$)$_2$] (**1**) with calculated IR acts.

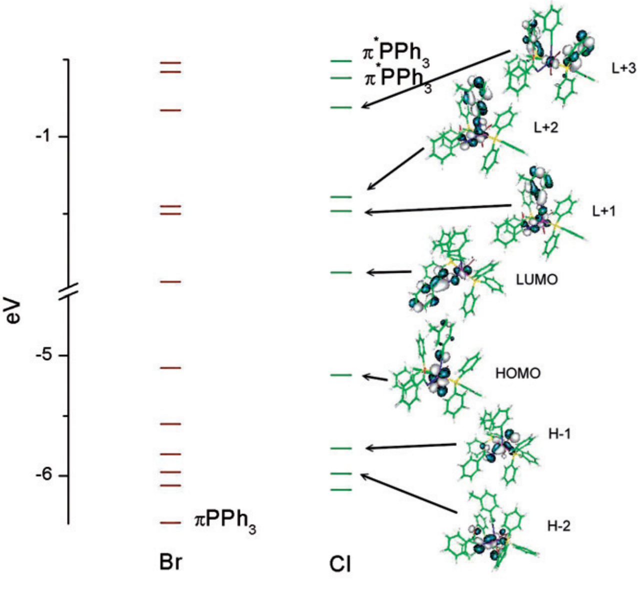

Figure 3. The simplified molecular orbital diagram of the complexes.

occupied molecular orbitals (HOMOs) and are in the range from HOMO–1 to HOMO–3. These molecular orbitals are mixed with π orbitals of the benzoyldiazenido and chloride/bromide. The $d_{x^2-y^2}$ and d_{z^2} orbitals are visible in the lowest unoccupied molecular orbital (LUMO) and LUMO+1/+2 with an antibonding admixture of benzoyldiazenido, halogen, and CH$_3$PhCN ligand orbitals. From figure 3 it may be concluded that the bromide complexes have a slightly smaller HOMO–LUMO gap (3.16 eV) than the chloride one (3.28 eV) which is connected with the difference in σ- and π-donor properties between these halides.

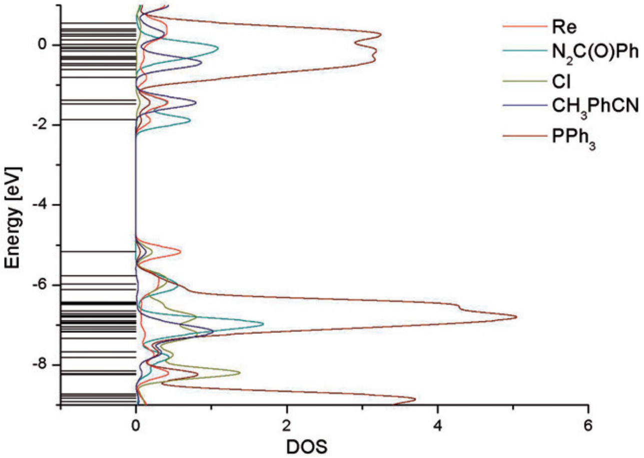

Figure 4. The DOS diagram for **1**.

In the frontier region, neighboring orbitals may show a quasi-degeneracy of the energy levels. In such cases consideration of only the HOMO and LUMO may not yield a realistic description of the frontier orbitals. For this reason partial DOS in terms of Mulliken population analysis were calculated using the GaussSum program. They provide a pictorial representation of the MO compositions and their contributions to chemical bonding. The DOS diagram for **1** is shown in figure 4. The DOS plot mainly presents the composition of the fragment orbitals contributing to the molecular orbitals. As may be seen from the DOS plot, the HOMOs have d_{Re} and p_{Cl} character with some contribution of π CH_3PhCN orbitals and the LUMOs are localized on d rhenium and π^* orbitals of the benzoyldiazenido ligands. The HOMO–1/–2/–3 are composed from the d_{Re},$\pi_{\mathrm{N_2C(O)Ph}}$, π orbitals of the triphenylphosphine ligands and p_{halogen}. In the LUMO+1/+2 the π orbitals of the CH_3PhCN ligands play a significant role (40–45%).

3.4. *Electronic spectra*

UV-Vis spectra of the complexes are similar and the maxima are located at 510, 378, 277, 250, 211 nm and 530, 382, 257, 211 nm for **1** and **2**, respectively. Assignments of the calculated transitions to the experimental bands are based on the criteria of energy and oscillator strength of the calculated transitions. In description of the electronic transitions only the main components of the molecular orbitals are taken into consideration. The electronic transitions were calculated with application of the CAM-B3LYP functional using the Coulomb-attenuating method.

Figure 5 presents the experimental and calculated electronic spectra of **1**. The first transitions (510 and 530 nm) in the spectra have HOMO → LUMO/LUMO+1 (90–83%) character. As the frontier HOMO and LUMO are localized on the d rhenium orbitals with an admixture of π X/$N_2C(O)Ph$ these transitions are associated with metal–ligand charge transfer (MLCT). The low intensity bands with maxima near 380 nm have the same character and the transitions between HOMO–3/–2 → LUMO

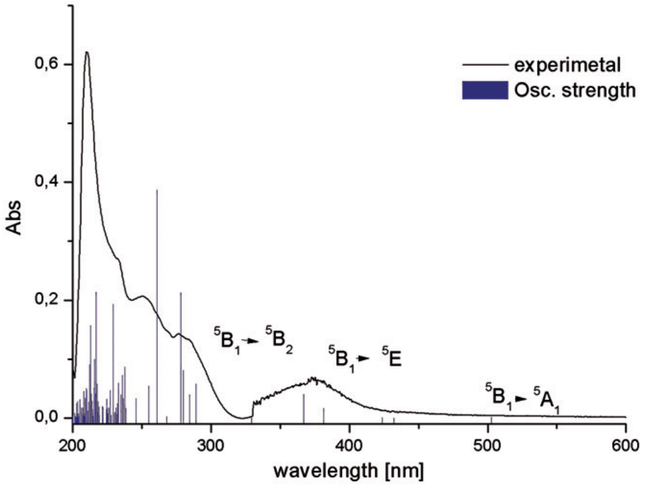

Figure 5. The experimental electronic spectrum of **1** with the calculated transitions.

Table 4. Calculated electronic transitions for **1** and **2** with the TDDFT method.

λ (nm)	Contributions	*f*	Experimental λ (nm)
	$[ReCl_2(N_2COPh)(CH_3PhCN)(PPh_3)_2]$ (**1**)		
502.6	HOMO → L + 1 (90%)	0.0013	510
423.8	HOMO → LUMO (83%)	0.0002	
381.3	HOMO–3/–2/–1 → LUMO (46%/14%/13%)	0.0166	378
367.1	HOMO → L + 2 (64%)	0.0403	
289.1	HOMO–2 → L + 1 (37%)	0.0576	
280.0	HOMO–2 → LUMO (44%); HOMO–1 → LUMO (23%)	0.081	
278.3	HOMO–2 → LUMO (16%); HOMO → L + 2 (46%)	0.1126	277
260.9	HOMO–15 → LUMO (16%); HOMO–3 → L + 1 (28%); HOMO–1 → LUMO (22%)	0.2872	
254.8	HOMO–1 → L + 3 (53%)	0.054	
217.0	HOMO–1 → L + 5 (15%); HOMO–8 → L + 1 (12%); HOMO–19 → LUMO (19%)	0.2137	211
	$[ReBr_2(N_2COPh)(CH_3PhCN)(PPh_3)_2] \cdot CH_2Cl_2$ (**2**)		
506.9	HOMO → L + 1 (90%)	0.0010	530
426.6	HOMO → LUMO (83%)	0.0007	
369.6	HOMO–3 → LUMO (29%); HOMO–2 → LUMO (21%)	0.0545	382
280.7	HOMO → L + 2 (59%)	0.2612	368
268.6	HOMO–3 → L + 1 (33%); HOMO → L + 2 (21%)	0.3693	
255.6	HOMO–4 → L + 1 (48%); HOMO–12 → LUMO (19%)	0.2616	257
229.8	HOMO–2 → L + 3 (26%)	0.1366	
218.2	HOMO–1 → L + 5 (46%); HOMO–5 → L + 4 (10%)	0.3284	
213.1	HOMO–2 → L + 7 (11%); HOMO–1 → L + 7 (14%)	0.2216	211

were calculated. The bands with maxima near 270 nm are attributed to transitions of ligand–metal charge transfer (LMCT) and MLCT types. The highest energy bands with maxima near 200 nm are attributed to transitions of ligand–ligand charge transfer type ($\pi \rightarrow \pi^*_{C=N}$) with contribution of MLCT transitions. Table 4 presents the calculated transitions for **3** and **4**.

The shape of the UV-Vis spectra of the complexes is appropriate to the d^4 configuration of rhenium. In octahedral symmetry the ground ^5D term splits into ^5E and ^5T terms which in the lower symmetry (D_{2h}) of the complexes split into $^5B_1$, $^5A_1$, ^5E, and $^5B_2$ levels. In this manner the lowest energy band above 500 nm is assigned to the $^5B_1 \rightarrow {}^5A_1$ transition. The bands with maxima near 380 nm are assigned to $^5B_1 \rightarrow {}^5E$, and the $^5B_1 \rightarrow {}^5B_2$ transition corresponds to bands at 270 nm. The ligand field parameters $10\,D_q$ are equal to 19,608 cm^{-1} and 18,868 cm^{-1} for **1** and **2**, respectively.

Supplementary material

CCDC 813589 and CCDC 813272 contain the supplementary crystallographic data for $[ReCl_2(N_2COPh)(CH_3PhCN)(PPh_3)_2]$ and $[ReBr_2(N_2COPh)(CH_3PhCN)(PPh_3)_2] \cdot CH_2Cl_2$. These data can be obtained free of charge from http://www.ccdc.cam.ac.uk/conts/retrieving.html, or from the Cambridge Crystallographic Data Centre, 12 Union Road, Cambridge CB2 1EZ, UK; Fax: (+44) 1223-336-033; or E-mail: deposit@ccdc.cam.ac.uk.

Acknowledgments

The Gaussian 09 calculations were carried out in the Wrocław Centre for Networking and Supercomputing, WCSS, Wrocław, Poland (http://www.wcss.wroc.pl grant number 18).

References

[1] U. Abram. In *Comprehensive Coordination Chemistry*, J.A. McCleverty, T.J. Meyer (Eds), Vol. 5.3, 2nd Edn, p. 271, Elsevier, Amsterdam (2003).
[2] J.L. Gal, M. Gonera, M.A. Lelait, D. Servent, Ch. Dugave. *J. Inorg. Biochem.*, **105**, 880 (2011).
[3] M. Aufort, M. Gonera, M.A. Lelait, B. Czarny, L.L. Clainche, R. Thaï, A. Landra, M.R. de Brimont, Ch. Dugave. *Eur. J. Med. Chem.*, **46**, 1779 (2011).
[4] S. Thiemea, S. Agostinib, R. Bergmanna, J. Pietzscha, H.J. Pietzsch, D. Cartab, N. Salvareseb, F. Refoscoc, C. Bolzatib. *Nucl. Med. Biol.*, **38**, 399 (2011).
[5] L. Huang, H. Zhu, Y. Zhang, X. Xu, W. Cui, G. Yang, Y.M. Shen. *Steroids*, **75**, 905 (2010).
[6] M. Teresa, A.R.S. da Costa, M. da Fátima, C.G. da Silva, J.J.R. Fraústo Da Silva, A.J.L. Pombeiro. *Collect. Czech. Chem. Commun.*, **72**, 599 (2007).
[7] H. Zollinger. *Diazo Chemistry II*, VCH, Weinheim, Germany (1995).
[8] J.R. Dilworth, P. Jobanputra, J.R. Miller, S.J. Parrott, Q. Chen, J. Zubieta. *Polyhedron*, **317**, 513 (1993).
[9] E.C.B. Alegria, M.V. Kirillova, L.M.D.R.S. Martins, A.J.L. Pombeiro. *Appl. Catal. A – Chem.*, **317**, 43 (2007).
[10] J.R. Dilworth, A. Desai, R.M. Thompson. *J. Mol. Catal. A – Chem.*, **115**, 73 (1997).
[11] S. Michalik, B. Machura, R. Kruszynski, J. Kusz. *J. Coord. Chem.*, **61**, 1066 (2008).
[12] J. Chatt, J.R. Dilworth, G.J. Leigh, V.P. Gupta. *J. Chem. Soc. A*, 2631 (1971).
[13] M.J. Frisch, G.W. Trucks, H.B. Schlegel, G.E. Scuseria, M.A. Robb, J.R. Cheeseman, G. Scalmani, V. Barone, B. Mennucci, G.A. Petersson, H. Nakatsuji, M. Caricato, X. Li, H.P. Hratchian, A.F. Izmaylov, J. Bloino, G. Zheng, J.L. Sonnenberg, M. Hada, M. Ehara, K. Toyota, R. Fukuda, J. Hasegawa, M. Ishida, T. Nakajima, Y. Honda, O. Kitao, H. Nakai, T. Vreven, J.A. Montgomery Jr, J.E. Peralta, F. Ogliaro, M. Bearpark, J.J. Heyd, E. Brothers, K.N. Kudin, V.N. Staroverov, R. Kobayashi, J. Normand, K. Raghavachari, A. Rendell, J.C. Burant, S.S. Iyengar, J. Tomasi,

M. Cossi, N. Rega, J.M. Millam, M. Klene, J.E. Knox, J.B. Cross, V. Bakken, C. Adamo, J. Jaramillo, R. Gomperts, R.E. Stratmann, O. Yazyev, A.J. Austin, R. Cammi, C. Pomelli, J.W. Ochterski, R.L. Martin, K. Morokuma, V.G. Zakrzewski, G.A. Voth, P. Salvador, J.J. Dannenberg, S. Dapprich, A.D. Daniels, O. Farkas, J.B. Foresman, J.V. Ortiz, J. Cioslowski, D.J. Fox. *Gaussian 09, Revision A.1*, Gaussian, Inc., Wallingford, CT (2009).

[14] A.D. Becke. *J. Chem. Phys*., **98**, 5648 (1993).

[15] C. Lee, W. Yang, R.G. Parr. *Phys. Rev. B*, **37**, 785 (1988).

[16] M.E. Casida. In *Recent Developments and Applications of Modern Density Functional Theory, Theoretical and Computational Chemistry*, J.M. Seminario (Ed.), Vol. 4, p. 391, Elsevier, Amsterdam (1996).

[17] T. Yanai, D. Tew, N. Handy. *Chem. Phys. Lett*., **393**, 51 (2004).

[18] P.J. Hay, W.R. Wadt. *J. Chem. Phys*., **82**, 299 (1985).

[19] N.M. O'Boyle, A.L. Tenderholt, K.M. Langner. *J. Comp. Chem*., **29**, 839 (2008).

[20] A.L. Tenderholt. *QMForge (Version 2.1)*, Stanford University, Stanford, CA, USA (2007).

[21] O.V. Dolomanov, L.J. Bourhis, R.J. Gildea, J.A.K. Howard, H. Puschmann. *J. Appl. Cryst*., **42**, 339 (2009).

[22] G.M. Sheldrick. *Acta Cryst*., **A64**, 112 (2008).

[23] T. Nicholson, J. Zubieta. *Polyhedron*, **7**, 171 (1988).

[24] S. Michalik, J.O. Dzięgielewski, R. Kruszynski. *J. Coord. Chem*., **58**, 1493 (2005).

[25] B. Machura, M. Wolff, I. Gryca. *Polyhedron*, **30**, 142 (2011).

[26] B. Machura, M. Wolff, R. Kruszynski, J. Mrozinski, J. Kusz. *Polyhedron*, **28**, 2377 (2009).

[27] A. Lazzaro, G. Vertuani, P. Bergamini, N. Mantovani, A. Marchi, L. Marvelli, R. Rossi, V. Bertolasi, V. Ferretti. *J. Chem. Soc., Dalton Trans*., 2843 (2002).

[28] L. Marvelli, N. Mantovani, A. Marchi, R. Rossi, M. Brugnati, M. Peruzzini, P. Barbaro, I. de los Rios, V. Bertolasi. *Dalton Trans*., 713 (2004).

[29] J. Chantler, P.E. Fanwick, R.A. Walton. *J. Organomet. Chem*., **604**, 219 (2000).

[30] P.K. Baker, M.G.B. Drew, M.M. Meehan. *Inorg. Chem. Commun*., **3**, 393 (2000).

[31] A.R. Cowley, J.R. Dilworth, P.S. Donnelly. *Inorg. Chem*., **42**, 929 (2003).